



OPEN ACCESS

EDITED BY

Luigi Jovane,
University of São Paulo, Brazil

REVIEWED BY

Jian Wang,
China University of Petroleum, China
Virsen Gaikwad,
Council of Scientific and Industrial
Research (CSIR), India
Ron Shaar,
Hebrew University of Jerusalem, Israel

*CORRESPONDENCE

Maryam A. Abdulkarim,
m.abdulkarim18@imperial.ac.uk

SPECIALTY SECTION

This article was submitted to
Sedimentology, Stratigraphy and
Diagenesis,
a section of the journal
Frontiers in Earth Science

RECEIVED 20 June 2022

ACCEPTED 01 August 2022

PUBLISHED 06 September 2022

CITATION

Abdulkarim MA, Muxworthy AR and
Fraser A (2022), High temperature
susceptibility measurements: A
potential tool for the identification of
oil-water transition zone in
petroleum reservoirs.
Front. Earth Sci. 10:973385.
doi: 10.3389/feart.2022.973385

COPYRIGHT

© 2022 Abdulkarim, Muxworthy and
Fraser. This is an open-access article
distributed under the terms of the
[Creative Commons Attribution License
\(CC BY\)](https://creativecommons.org/licenses/by/4.0/). The use, distribution or
reproduction in other forums is
permitted, provided the original
author(s) and the copyright owner(s) are
credited and that the original
publication in this journal is cited, in
accordance with accepted academic
practice. No use, distribution or
reproduction is permitted which does
not comply with these terms.

High temperature susceptibility measurements: A potential tool for the identification of oil-water transition zone in petroleum reservoirs

Maryam A. Abdulkarim^{1,2*}, Adrian R. Muxworthy¹ and
Alastair Fraser¹

¹Department of Earth Science and Engineering, Imperial College London, London, United Kingdom,

²Department of Petroleum Engineering, Baze University, Abuja, Nigeria

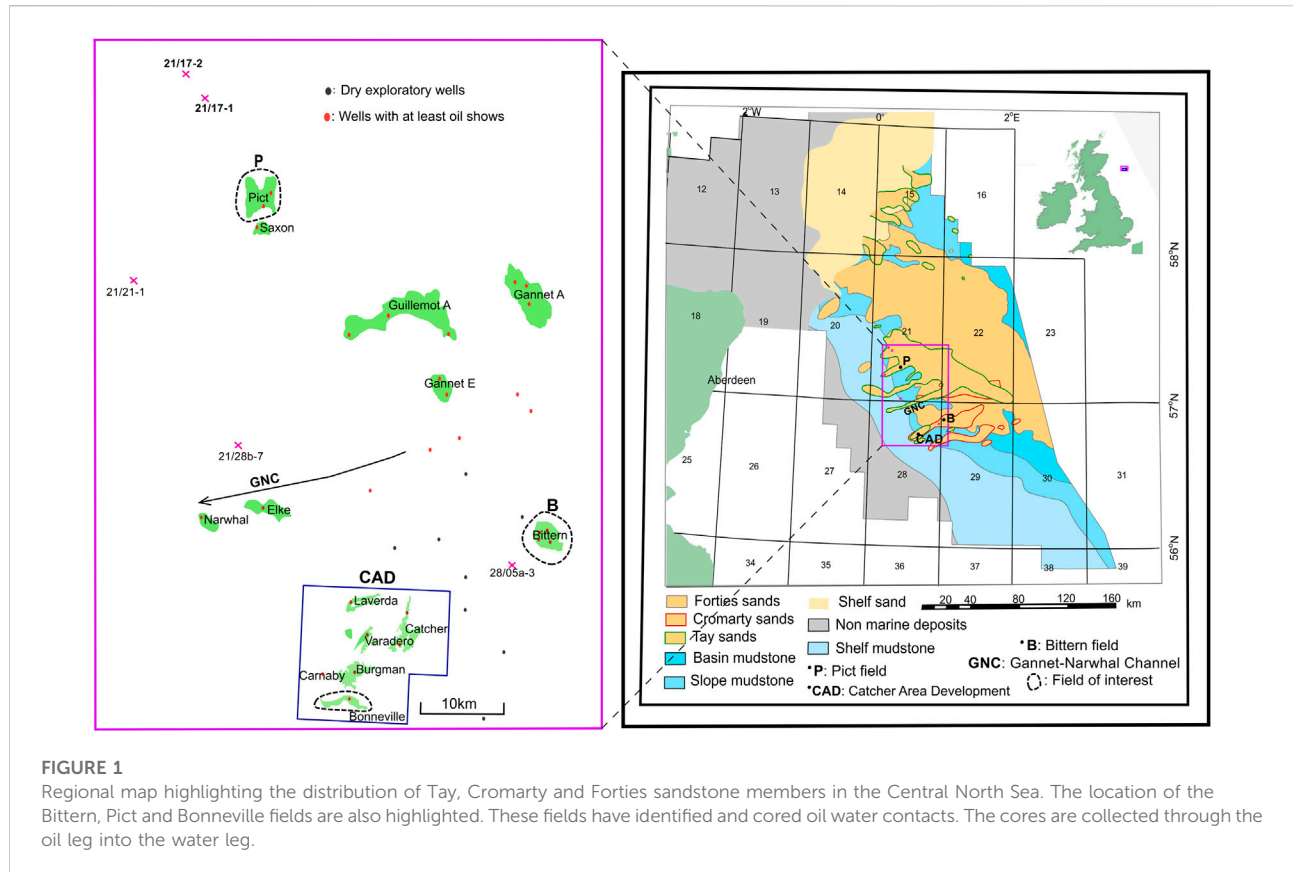
Determining the position and thickness of the oil-water transition zone (OWTZ) in hydrocarbon reservoirs is important to reserve estimation and production planning. This paper describes a magnetic method of identifying this zone. High temperature susceptibility (HT- χ) measurements on core samples from Paleogene reservoirs of the UK Central North Sea revealed distinct signatures around the oil water interface. Rapid increases in susceptibilities at temperatures <250°C were observed for samples around the oil water interface unlike the main oil leg where alteration involving increase in susceptibility occurred at significantly slower rates and higher temperatures. The HT- χ data together with Mössbauer measurements revealed that the variation in alteration characteristics is due to the increasing concentration of hexagonal pyrrhotite and/or lepidocrocite around the oil water interface. Hexagonal pyrrhotite was identified in reservoirs existing at temperatures of <80°C, while lepidocrocite dominated the signature around the contact of deeper reservoirs. These observations suggest that the precipitation of hexagonal pyrrhotite is related to OWTZ centred biogenic activities i.e., biodegradation. The dominance of lepidocrocite in deeper diagenetic settings has been related to hydrolysis of hydrocarbon at the oil water interface, together with cessation of biogenic activities.

KEYWORDS

magnetic mineral diagenesis, oil water contact, oil-water transition zone, magnetic method, UK Central North Sea, biodegradation, hydrolysis

1 Introduction

The oil-water transition zone (OWTZ) in a petroleum reservoir is the zone below the main oil leg where the saturation of water progressively increases from an irreducible value to 100% (Adegbite et al., 2021). The thickness of this transition zone is dependent on several properties including the hydrocarbon density, the reservoir pore sizes and



distribution *etc.*, and can range from a few metres to several hundreds of metres (Bera and Belhaj, 2016; Adegbite et al., 2021). In the main oil leg, only immovable water exists. Identifying each of these boundaries/zones is important to reserve estimation and production planning (Fanchi et al., 2002).

The OWTZ is known to be a zone of significant diagenesis, due to the presence of mobile hydrocarbons and formation water that can support several biogenic (Head et al., 2014) and thermogenic (Burton et al., 1993; Helgeson et al., 1993) processes. These processes have been shown to involve the formation, alteration and destruction of magnetic minerals (Head et al., 2010; Badejo et al., 2021b). The magnetic mineralogy of this region may therefore be variant from the overlying and underlying zones and could be identifiable through magnetic techniques (Badejo et al., 2021b; Abdulkarim et al., 2022b).

In this paper we propose the use of high-temperature magnetic susceptibility ($HT-\chi$) measurement as a method of distinguishing between the OWTZ and the main oil and water legs in petroleum reservoirs. This paper reports the distinguishing parameters determined through experimental measurements on core samples from Palaeogene petroleum reservoirs in the UK Central North Sea. This novel approach of determining OWTZ has the potential to be used alongside

standard core, log and pressure-based methods, each with their own uncertainties/limitations. Accuracy of magnetic methods will not be dependent on the mud type used. Also, it will be relatively cheaper than wireline based methods.

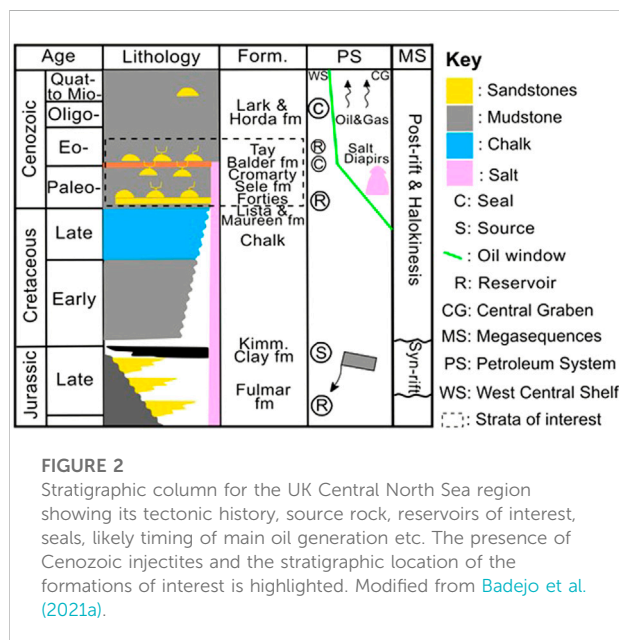
2 Geological setting of the study area

Cores from three hydrocarbon fields were sampled: the Bittern, Pict and Bonneville fields of the UK Central North Sea (Figure 1). These hydrocarbon fields are Cenozoic accumulations and contain hydrocarbon sourced from the type II Kimmeridge clay (Jurassic) source rock of the region (McKie et al., 2015). Their reservoir and hydrocarbon properties are detailed in Table 1.

The UK Central North Sea is part of the southern arm of a trilete Jurassic rift system that defines the structure of the UK Northern North Sea Basin (Fraser et al., 2003). The rift was formed by extension in the Late Jurassic resulting in an isolated and anoxic basin that supported the deposition and preservation of the Upper Jurassic Kimmeridge clay source rocks (Figure 2). The system returned to an oxic state in the Cretaceous period with the deposition of mudstone and chalk in a period of relative tectonic quiescent (Copestake et al.,

TABLE 1 Reservoir and fluid properties of the fields under study. pH data is available for the Bonneville field. The pH quoted for Pict was obtained from a nearby well in an adjoining block. There are no pH data for the Bittern field. MMbbl, bcf, MMboe and TVDSS stand for million barrels, billion cubic feet, million barrels of oil equivalent and true vertical depth subsea respectively. Compiled using data from literature (Ritchie et al., 2011; Tamannai et al., 2013) and wells.

	Bittern	Pict	Bonneville
Reservoir Sands	Forties, Cromarty	Tay	Tay
Reservoir Top TVDSS, m (ft)	2,020 (6,628)	1,578 (5,176)	1,049 (3,443)
Gross Pay, m (ft)	80 (246)	98 (322)	—
Av. Reservoir Temp, °C (°F)	90 (194)	66 (150)	46 (114)
Sulphur Content	Low	Low	Low
Stock Tank Density, °API	39	33	24
Gas oil contact (TVDSS), m (ft)	2,055 (6,742)	1,614 (5,296)	1,067 (3,502)
Oil water contact (TVDSS), m (ft)	2,103 (6,901)	1,647 (5,403)	1,090 (3,577)
STOIP, MMbbl	250	—	30
Gas initially in place, bcf	300	—	—
Est. Reserve, MMboe	—	15	—
Insitu oil degradation level	Non degraded	Slightly degraded	Moderately degraded
Acidity, pH	?	7?	7



2003; Surlyk et al., 2003; Johnson et al., 2005). The end of the Cretaceous is marked by the initiation of the Iceland hotspot at ~60 Ma leading to massive uplift of the northern UK and the shedding of large volumes of coarse grained material eastwards into the region (Ahmadi et al., 2003). These sediments include the Tay, Cromarty and Forties reservoir sandstones with accumulations sourced from the underlying Kimmeridge clay source rocks (Kubala et al., 2003).

The Tay, Cromarty and Forties sandstones form part of the Horda, upper Sele and the lower Sele formations of the Central North Sea respectively (Figure 2) (Ahmadi et al., 2003). The Sele formation which began deposition ~56 Ma, consists mainly of mudstones that are typically medium to dark grey, carbonaceous, commonly laminated and fissile. The Forties sandstone is fine to coarse grained, moderately to poorly sorted, and is interbedded with dark grey siltstones and mudstones (Ahmadi et al., 2003; Eldrett et al., 2015). This sandstone unit formed a north-westerly to south-easterly trending lobe with smaller west-south-west (WSW)—east-north-east (ENE) slope channels and deep basin deposits (Robertson et al., 2013; Mudge, 2015). The Forties sandstone is present in the Bittern field but thins rapidly to the west and is absent in the Bonneville and Pict fields. The overlying and less extensive Cromarty sandstone of the upper Sele formation was sourced from the Forties platform and deposited in the region as isolated near W-E slope channels and slump/debris flow deposits (Figure 1) (Robertson et al., 2013; Mudge, 2015). Compared to the Forties channels, the Cromarty sandstone extends further west in the region and is present in the Bittern and Bonneville fields. It is made up of fine grained clean poorly consolidated sands that are interbedded with grey carbonaceous mudstone (Ahmadi et al., 2003). Overlying the Sele formation is the Horda formation comprising a thick sequence of green to grey hemipelagic mudstones together with the coarse grained poorly consolidated Tay sandstone (Jones et al., 2003). The Tay sandstone was deposited on a Horda formation that was unconformable due to salt induced highs and lows, and the

TABLE 2 Details of the cores sampled for this study. N/G stands for net (sandstone) to gross (sediments).

Field	Bittern		Pict		Bonneville
Well	29/01a-7	29/1b-5	21/23b-1	21/23b-6	28/09a-6
Core Length, m (ft)	80 (261)	35 (115)	61 (199)	19 (62)	26 (84)
N/G (%)	~90	~90	~100	~80	~50
Sample number	39	16	26	9	20

presence of Tertiary faults (Stewart, 1996; Jones et al., 2003). This together with the diminished sediment supply to the region resulted in slope deposits that accumulated mainly in areas of tectonically induced lows, e.g., the hanging walls of the Tertiary faults (Robertson et al., 2013). The Tay sandstone is found in the Bonneville and Pict field and does not extend into the deeper Bittern area.

3 Experimental methodology

3.1 Sample collection

Sandstone samples from cores of the Bittern, Pict and Bonneville fields were obtained at the British Geological Survey Core Store, Keyworth, (UK) (Table 2). These cores were obtained from the oil leg through to the water leg. The Bonneville field was sampled every metre. Due to the length of the Bittern and the Pict fields' cores, sampling was performed approximately every 2 m. Smaller sampling spacing was used in areas of observed heterogeneity and around known hydrocarbon-fluid contacts.

3.2 High temperature susceptibility measurement

The HT- χ experiments measures the magnetic susceptibility (χ) of the samples as they are heated in Argon from room temperature to 700°C and back. This enables the identification of magnetic minerals through their phase transitions or their alteration characteristics, e.g., a rapid increase in magnetic susceptibility of hexagonal pyrrhotite as it alters and becomes ferrimagnetic at about 200°C, with a Curie temperature of 265°C (Rochette et al., 1990).

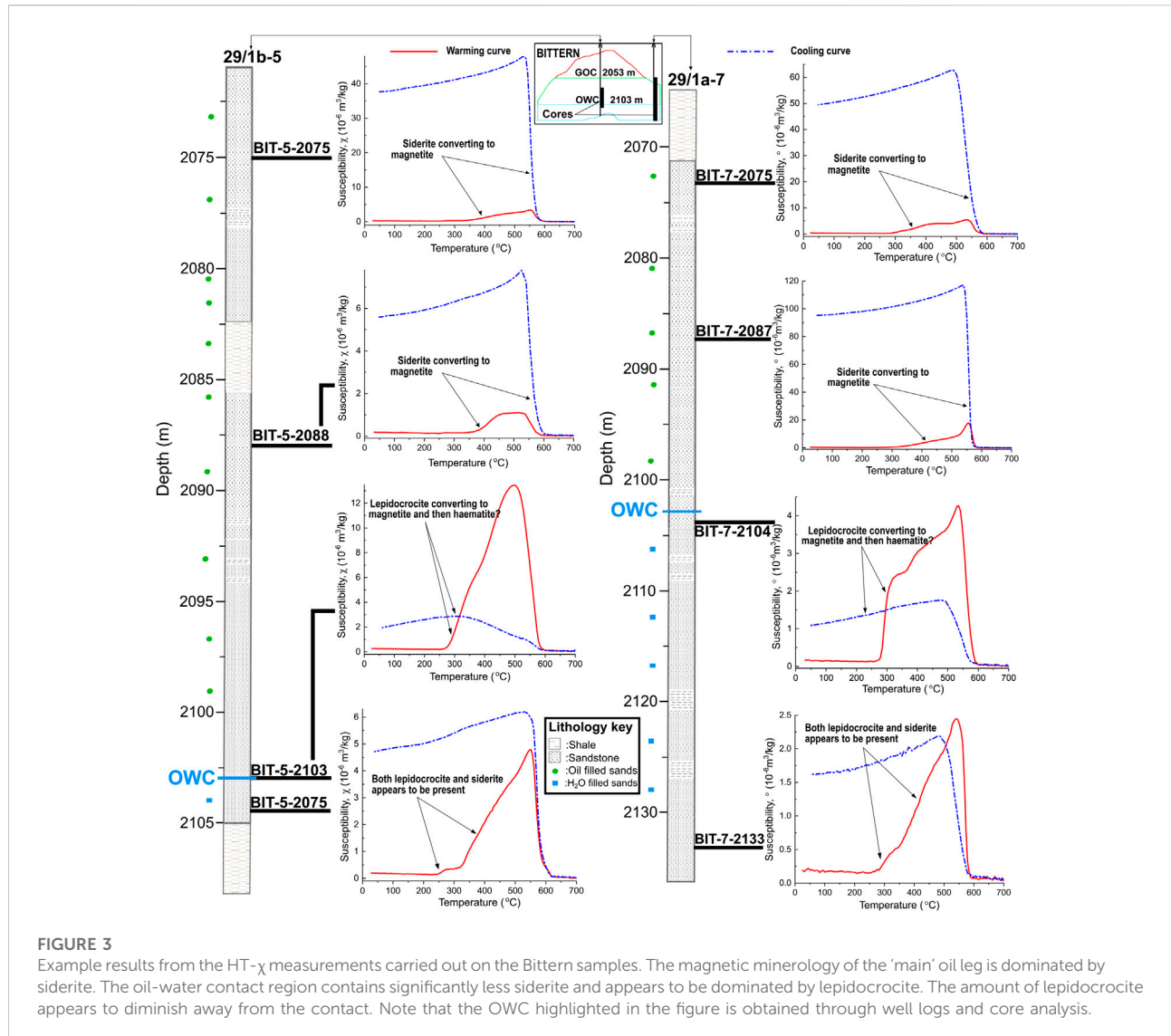
An MFK1-FA Agico Kappabridge was used at Imperial College London. Between 0.4 and 0.5 g of a sample was measured and poured into a clean and dry test tube. This was then placed in the instrument for measurement. Magnetic susceptibility measurements were made every ~5°C on heating and cooling. A fast heating/cooling rate of approximately 14°C/min was applied. To determine the background signal, an empty sample holder was measured using the same experimental sequence.

3.3 Mössbauer spectroscopy

To verify the magnetic mineralogy, Mössbauer spectra were measured for three samples from the OWTZ. This measurement was carried out at the Institute of Rock Magnetism (The IRM), University of Minnesota, USA. Due to the low concentration of magnetic minerals present (<< 1%), magnetic separation was carried out before Mössbauer spectra measurement. A S. G. Frantz Co. Inc. Frantz magnetic separator (model LB-1) at Imperial College London was used for this purpose.

The samples were crushed using a mortar and pestle to less than 100 μm in diameter. This is helpful in separating the non-magnetic particles from the magnetic particles. To achieve magnetic separation, a sample was placed in the hopper of the Frantz magnetic separator with its outlet plugged. The magnetic power supply was turned on followed by the feed and chute controllers. The hopper was unplugged, and the controllers increased gradually from zero leading to the sample gradually moving along the chute and separating into the magnetic or non-magnetic fractions. For the initial run per sample, a current of 0.01 mA was applied to obtain the starting field strength. The current was progressively increased to 0.03, 0.05, 0.1, 0.2, 0.3 and 0.5 mA in subsequent runs to optimize the extraction process and limit the loss of any magnetic mineral. Excessive feed rates and chute vibration that results in inefficient separation was avoided. This was determined visually. At the end of each separation, the whole set-up was vacuumed and sprayed with compressed air to avoid contamination between samples. Note that selecting the optimal setting is highly sample dependent, more details on this process may be found in Rosenblum and Isabelle, (n.d.).

⁵⁷Fe Mössbauer spectra were measured with an MS6 spectrometer, using Janis SVT-400 Nitrogen-shielded liquid Helium cryostat with a constant acceleration drive and a 512-multichannel analyser. A liquid Helium cryostat was available to allow spectra to be recorded down to 5 K. This was useful in assessing the presence of paramagnetic minerals that become ferromagnetic at low temperatures e.g., siderite and lepidocrocite. With respect to preparations, the samples were pressed inside a standard circular Mössbauer holder (diameters ~



1.3 cm). The measurement time was between several hours to up to 1 day. Results are given with reference to metallic iron. The spectra were analysed by means of a least-squares fitting procedure using Lorentzian line shapes.

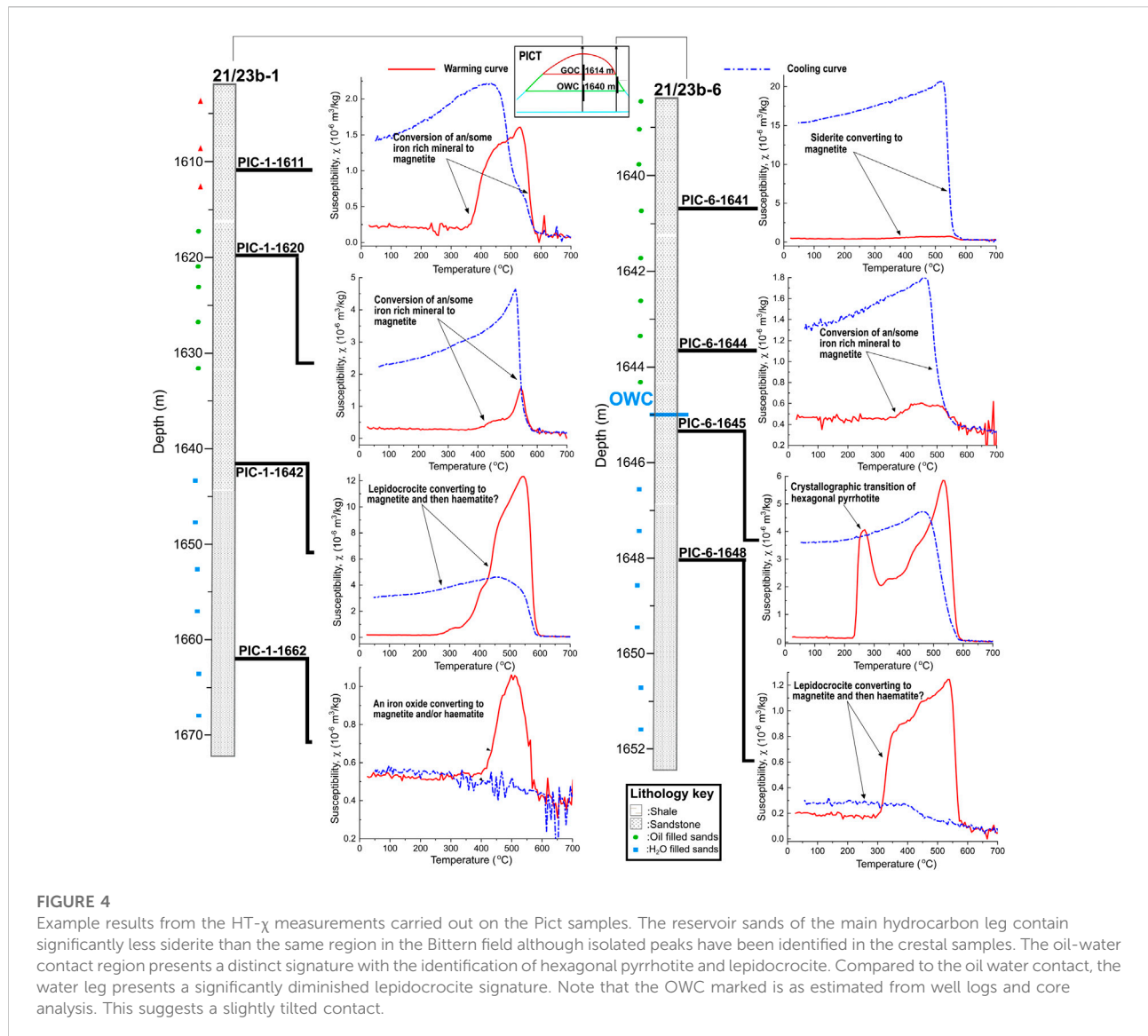
4 Results

4.1 High-temperature susceptibility measurements

4.1.1 The Bittern field

HT- χ curves for the Bittern samples from the oil leg and the water leg generally display increase in susceptibility above 300°C with Curie temperatures of between 560 and 580°C, e.g., BIT-5-

2075 and BIT-7-2087 (Figure 3). Further increase in susceptibility is generally observed on cooling from 580°C. This suggests significant alteration of iron containing minerals specifically siderite to magnetite (Pan et al., 2000). The rate and/or magnitude of the increase in susceptibility for these samples varies significantly e.g., BIT-5-2088 and BIT-7-2075's final susceptibilities on their cooling curves are respectively ~30 and 500 times greater than the initial susceptibilities measured on the heating curve (Figure 3). Hopkinson peaks with varied signatures are also observed e.g., BIT-7-2075 and BIT-7-2087 (Figure 3). Less than 5% of the oil leg's sandstones samples display no alteration. The unaltered samples present with Curie temperature of ~580°C suggesting the presence of original magnetite. Similar signatures have been observed in oil leg core samples from the Gannet and Guillemot fields, UK Central North Sea (Badejo et al., 2021c).



Samples close to the oil water contact exhibit a rapid and/or near instantaneous increase in susceptibility at about 270°C on the heating curve with Curie temperature of about 580°C e.g., BIT-5-2,103 and BIT-7-2,104 (Figure 3). These samples' cooling curves generally present a reduction in susceptibility when compared to the maximum value obtained from the heating run. This signature appear to suggest the presence of lepidocrocite (Gehring and Hofmeister, 1994; Gendler et al., 2005). Although, some samples from the oil leg display some element of this signature, the inferred magnitudes of lepidocrocite are comparatively insignificant to that of the near oil water contact samples.

4.1.2 The Pict field

Similar to the Bittern field, the HT- χ curves for the Pict samples from the oil leg and the water leg exhibit increases in

susceptibility from about 300°C on warming, a Hopkinson peak at around 550°C and a subsequent Curie temperature siderite to magnetite (Pan et al., 2000). Further increases in susceptibility are commonly observed on cooling (Figure 4). There also appear to be some original magnetite in these samples albeit minimal. The HT- χ curves for samples around the oil-water contact which were taken from two different locations, well 21/23b-1 and well 21/23b-6, exhibit different signatures (Figure 4). The curves for samples from well 21/23b-6 display a rapid and near instantaneous increase in susceptibility at about 230°C with a Curie temperature of approximately 270°C e.g., PIC-6-1,645, suggesting hexagonal pyrrhotite (Rochette et al., 1990). There was further increase in susceptibility above 300°C with a Curie temperature of about 580°C. The susceptibilities observed for the cooling curves of these samples are generally less than the

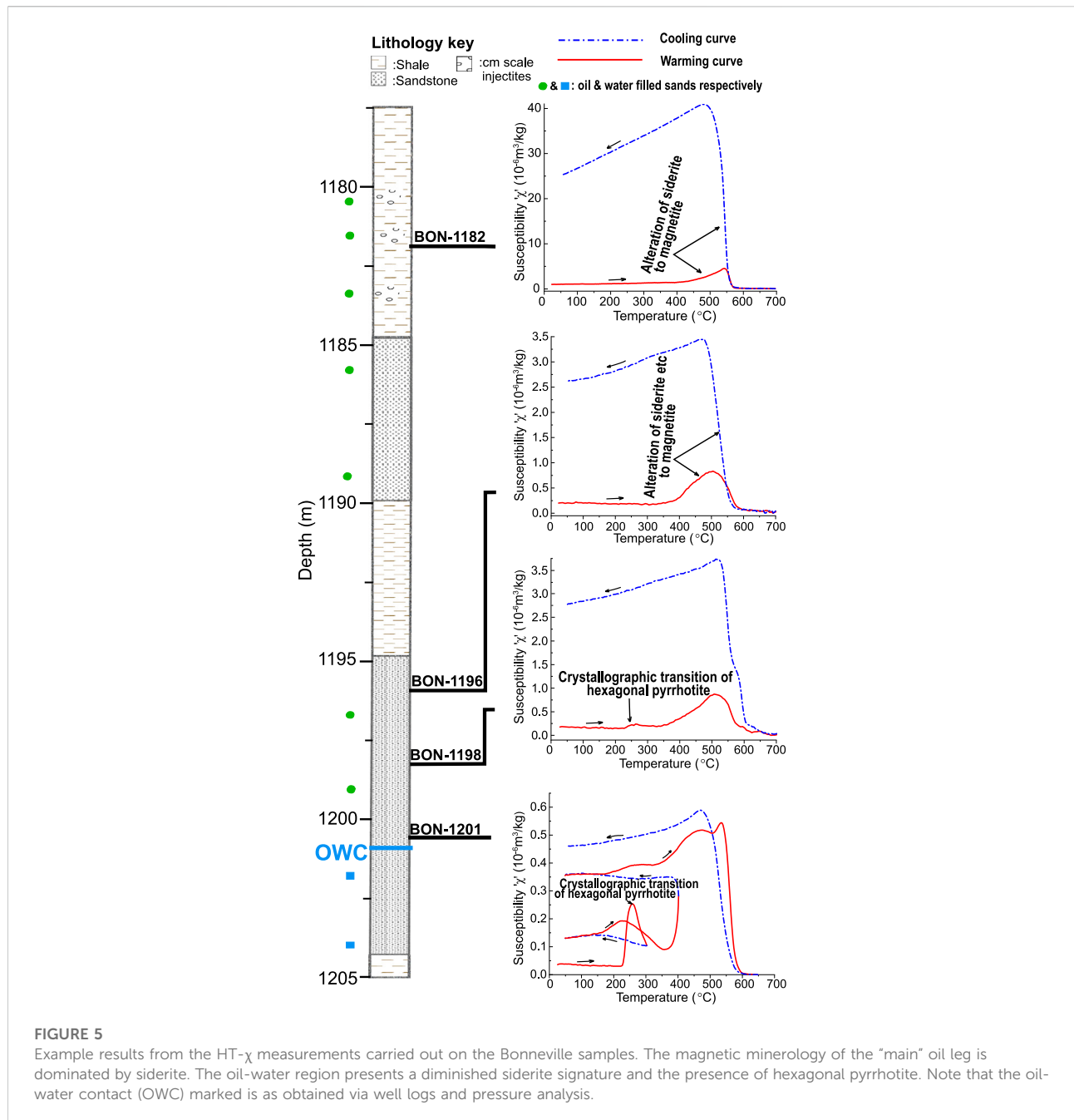


FIGURE 5

Example results from the HT- χ measurements carried out on the Bonneville samples. The magnetic mineralogy of the "main" oil leg is dominated by siderite. The oil-water region presents a diminished siderite signature and the presence of hexagonal pyrrhotite. Note that the oil-water contact (OWC) marked is as obtained via well logs and pressure analysis.

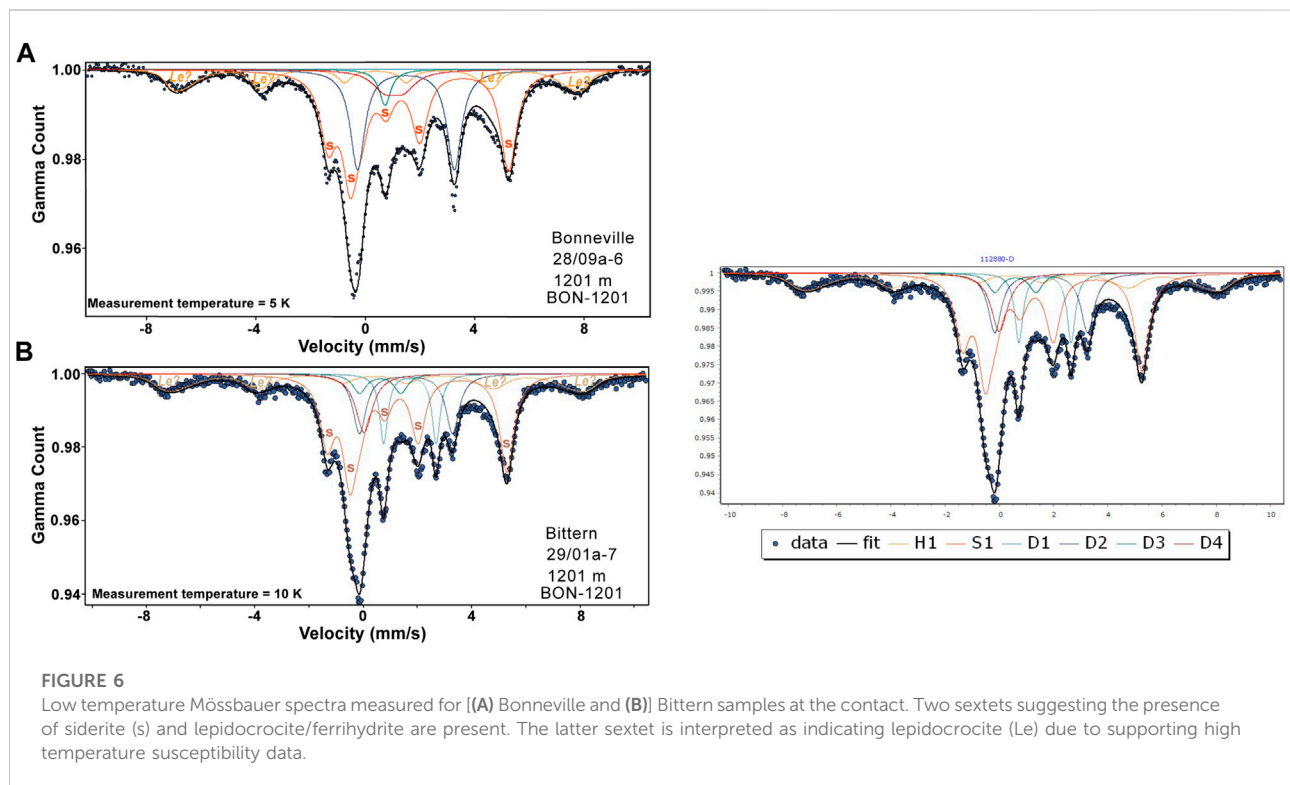
maximum value observed on the heating curves. For the samples from well 21/23b-1, the susceptibility trend observed is similar to the signature of the samples from the vicinity of the OWC of the Bittern field i.e., a rapid increase in susceptibility at about 280°C with a Curie temperature of about 580°C e.g., PIC-1-1,642. The susceptibility trend of the cooling curve is also less than the maximum susceptibility of the warming curve. This suggests the presence of lepidocrocite (Gehring and Hofmeister, 1994; Gendler et al., 2005).

4.1.3 The Bonneville field

Similar to the Bittern and Pict fields, the Bonneville oil leg samples' HT- χ curves generally exhibit an increase in susceptibility from above 300°C with Curie temperature of between 560 and 580°C signifying the alteration of iron rich minerals to magnetite e.g., BON-1182 and BON-1196 (Figure 5). Hopkinson peaks are also observed in most of these samples. Further increases in susceptibilities are observed in the cooling curve. The samples from the vicinity

TABLE 3 Mössbauer parameters for the samples around the OWC. IS stands for isomer shift, QS stands for quadrupole splitting and B_{hf} stands for the magnetic hyperfine field. *Lepi and ferri* stands for lepidocrocite and ferrihydrite. Data from Dyar et al. (2006); Stevens et al. (2005) are applied to mineral interpretation.

sample location/ sample name		temp (K)	IS (mm/s)	QS (mm/s)	B_{hf} (T)	mineral interpretation
Bittern	doublet I	295	1.22	1.84		siderite
Bit-7-2104	doublet II		0.32	0.65		pyrite? lepi? ferri etc
Pict	doublet I	295	1.21	1.83		siderite
Pic-6-1645	doublet II		0.34	0.64		pyrite? lepi? ferri etc
Bonneville	doublet I	295	1.26	1.81		Siderite silicate? lepi? ferri etc
Bon-1201	doublet II		0.42	0.57		
Bittern	sextet II	10	0.41	0.04	49.4	lepi? ferri?
Bit-7-2104	sextet I		1.34	2.05	17.9	siderite
Bonneville	sextet II	5	0.42	0.08	47.3	lepi? ferri?
Bon-1201	sextet I		1.34	2.03	17.9	siderite



of the oil water contact exhibit a variant signature. A rapid and near instantaneous increase in susceptibility is observed at about 230°C with a Curie temperature of about 280°C, e.g., BON 1201 (Figure 5). This suggests the presence of hexagonal pyrrhotite (Rochette et al., 1990). Further increases in susceptibility above 300°C and a Curie temperature of about 580°C is also observed (Figure 5).

4.2 Mössbauer results

The Mössbauer spectra were obtained at room and low temperatures (either at 5 and 10 K) and analysed by a fitting procedure using Lorentzian curves (Dyar et al., 2006). These spectra present a good fit with two doublets that realign due to magnetic ordering at low temperature to produce two magnetic

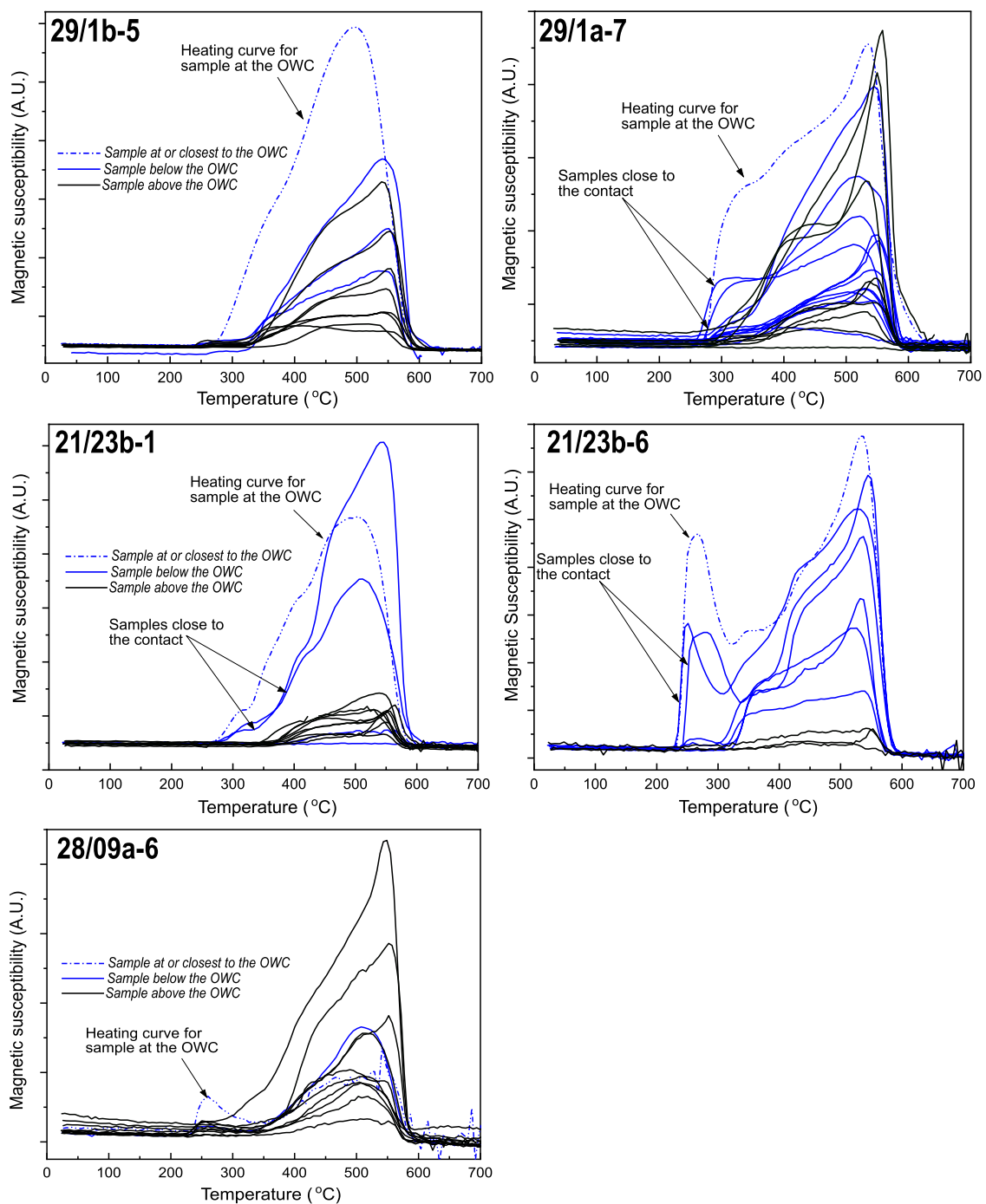


FIGURE 7

Overlaying the heating curves obtained per well. This emphasizes the differences in magnitude and trend of susceptibility as observed for the near OWC samples and those from the oil and water legs.

hyperfine sextet (Table 3). The isomer shift (IS) and quadrupole splitting (QS) for doublet I at room-temperature in all three samples strongly suggest the presence of siderite (Stevens et al., 2005; Dyar

et al., 2006). For doublet II, the IS and QS values suggest the presence of lepidocrocite, ferrihydrite, pyrite or even a silicate (Figure 6). At low temperatures, the IS, QS and magnetic hyperfine field (B_{hf}) for

sextet I strongly suggests the presence of siderite in all the samples. For the less well defined sextet II, the parameter's values suggest the presence of lepidocrocite or ferrihydrite, plus possibly even magnetite or maghemite, though B_{hf} is a little low (Stevens et al., 2005). Combining the interpretation for doublet II and sextet II suggest that the most likely mineral is lepidocrocite or ferrihydrite. The wide range in IS, QS and B_{hf} values observed between samples is not unusual for lepidocrocite and ferrihydrite; Stevens et al. (2005) collated the values obtained for these parameters in a significant number of Mössbauer studies; IS, QS and B_{hf} values ranged between 0.32–0.57 mm/s, - 0.05–0.05 mm/s, and 42–50 T respectively. The wide range of values observed is likely due to poor crystallinity, structural variations or defect and impurities in material which are hard to synthesise (Hirt et al., 2002; Dyar et al., 2006).

5 Discussion

Variations in the high temperature susceptibility (HT- χ) curves for sandstones of the oil-water transition zone (OWTZ) and the oil leg region of some petroleum reservoirs have been identified. HT- χ together with Mössbauer measurements suggest that the sandstone of the OWTZ is significantly richer in magnetic minerals such as hexagonal pyrrhotite and/or lepidocrocite making its alteration characteristics on heating different from sandstones of the oil leg. The oil leg appears to be rich in mainly siderite and/or magnetite. The water leg compared to the OWTZ is low in lepidocrocite and hexagonal pyrrhotite. The comparative alteration characteristics for sandstones from the OWTZ and the main oil and water legs presents with inter and even intra reservoir variations (Figures 2–4, Figure 6). However, a common feature observed for the sandstones of the OWTZ is alteration onset at lower temperatures (Figure 7).

5.1 Magnetic mineral diagenesis at the OWTZ

The OWTZ is a region of significant diagenesis (Head et al., 2014; Pannekens et al., 2019). The type of diagenetic activities taking place depends on several factors including the depth of the reservoir especially whether it is below or above the biodegradation threshold, the constituent of the hydrocarbons, the formation water salinity, the rock mineralogy etc. Magnetic mineral diagenesis will therefore also be variant depending on these properties (Burton et al., 1993; Roberts, 2015). Below we discuss the formation conditions of the magnetic minerals identified.

5.1.1 Formation of hexagonal pyrrhotite

The HT- χ data from the Bonneville and Pict fields have shown that hexagonal pyrrhotite may precipitate at the OWTZ in

a clastic system. The requirements for its formation and preservation include the presence of limiting amount of sulphide, excess reactive iron and labile organic carbon content (Kao et al., 2004). These conditions very likely exist in the region as inferred from the well data (Table 1). We also note the absence of hexagonal pyrrhotite in the Bittern field. This together with the mineral's prevalence around the OWTZ of the Pict and Bonneville fields, the reservoirs' temperatures, and the degradation levels of the oils (Table 1) suggest that its precipitation is related to biodegradation of hydrocarbon. Biodegradation of hydrocarbons predominantly occur at temperatures <80°C, and at the OWTZ due to the presence of mobile water supplying nutrients and a carbon source (oil) all of which are essential for the microorganisms responsibly for degradation to thrive (Head et al., 2014; Pannekens et al., 2019). The degradation pathway in the reservoirs of interest likely involves anaerobic sulphate reduction which supplies the essential sulphide that combines with available Fe^{2+} in an environment made geochemically suitable for the formation of hexagonal pyrrhotite by the presence of hydrocarbons (Kao et al., 2004). Away from the contact, sulphide ion concentration diminishes rapidly. Consequently, anaerobic sulphate reduction ceases, enabling the siderite in the main oil leg.

Reactions between iron and sulphur lead to the formation of pyrite, greigite and/or pyrrhotite (Roberts and Turner, 1993; Kao et al., 2004). Pyrrhotite and greigite are known to be unstable in the presence of excess H_2S transforming eventually to pyrite (Kao et al., 2004); we infer that it is more likely to preserve pyrrhotite and greigite in low sulphur hydrocarbon reservoir systems (Table 1). The thermodynamic requirements for the formation and preservation of pyrrhotite and greigite in a low sulphur environment are different. (Kao et al., 2004). Although, due to the complexity of the processes, there is a dearth of studies that describe in specifics, deep geological environments tied to geochemical conditions, where each of these iron sulphides will be stable. However, comparative descriptions of their thermodynamic requirements are available (Burton et al., 1993; Kao et al., 2004). Thermodynamic and experimental studies suggest that compared to pyrrhotite, greigite requires a lower supply of labile organic matter, higher supply of reactive iron, lower sulphide concentration and finer grained sediments (Kao et al., 2004). Pyrrhotite and greigite have also been identified in sandy and muddy sediments respectively of the same stratigraphic level (Roberts and Turner, 1993; Abdulkarim et al., 2022b). We can infer from these studies that the precipitation of pyrrhotite at OWTZ is probable as this zone usually falls within sandy intervals in petroleum reservoirs.

5.1.2 Formation of lepidocrocite

Lepidocrocite has been identified in significantly higher quantities around the OWC as compared to the oil and water legs of the Pict and Bittern fields (Figures 3, 4, Figure 7). The formation of lepidocrocite is generally attributed to shallow

diagenetic processes taking place in oxic/sub oxic environments (Hirt et al., 2002; Liu et al., 2014; Roberts, 2015). However, this study suggests that it can form at greater depths. Its formation appears to be centred at the OWTZ suggesting that the presence of mobile water and hydrocarbons has significant impact on the process. Helgeson et al. (1993) proposed that at the oil water interface in deep petroleum reservoirs, significant hydrolysis of hydrocarbons occur. This process can lead to the formation of lepidocrocite if the other geochemical requirements are present (Fu et al., 2011; Bassez, 2017).

The geochemical requirements for the formation of lepidocrocite include a near neutral pH, a non-sulphidic environment and the presence of available iron (Gendler et al., 2005; Roberts, 2015). In a sulphidic environment, iron sulphide(s) will preferentially precipitate (Burton et al., 1993; Roberts, 2015; Badejo et al., 2021c). This likely accounts for the dominance of lepidocrocite at the OWTZ of the Bittern sands and its diminishing signature in the Pict and Bonneville sands. The latter two sands contain hydrocarbons that have undergone in-reservoir degradation, a process via which sulphide ions may be produced. Available sulphide ions will react with Fe^{2+} in these systems and only after it is consumed will the precipitation of lepidocrocite be possible (Roberts, 2015).

How universal will the precipitation of lepidocrocite at the OWTZ be? The results here suggest that the precipitation of lepidocrocite will be more likely in low sulphur reservoir systems existing at temperatures greater than the threshold for biodegradation ($>80^\circ\text{C}$).

5.2 Differential alteration characteristic of the sandstones from the OWTZ–reaction mechanism

The magnetic signatures of the hydrocarbon reservoirs are complex and variant (Reynolds et al., 1990; Liu et al., 2006; Emmerton et al., 2013; Roberts, 2015; Abubakar et al., 2020; Badejo et al., 2021a, 2021b; Abdulkarim et al., 2022b, 2022a). The behaviour of oil-stained sandstones when heated will also be variant even within the oil leg, OWTZ and water leg. In this paper, we find that the differentiating parameter in the HT- χ curves is mainly due to the low alteration temperature of lepidocrocite and hexagonal pyrrhotite. Hexagonal pyrrhotite undergoes a unique crystallographic transition (also known as λ -transition) at temperatures ' T_λ ' of $200\text{--}220^\circ\text{C}$ from its antiferromagnetic state to a ferrimagnetic form (Hornig, 2018). The ferrimagnetic phases has a Curie temperature of $275\text{--}295^\circ\text{C}$ (Rochette et al., 1990) and is preserved when cooled below T_λ (Figure 5). We observed a T_λ of $\sim 230^\circ\text{C}$ for our samples which is slightly higher than the reported range. The Curie temperature of the new formed ferrimagnetic product however falls within the quoted range. The high T_λ observed is possibly due to a slight deviation in stoichiometry (Dekkers, 1989).

Lepidocrocite has been shown to undergo rapid increase in susceptibility beginning at $200\text{--}250^\circ\text{C}$ as a result of its transformation to maghemite (Gehring and Hofmeister, 1994; Gendler et al., 2005). Around this temperature, the hydroxyl bond in lepidocrocite ($\gamma\text{-FeOOH}$) is broken, and the resulting ions structurally transforms to maghemite ($\gamma\text{-Fe}_2\text{O}_3$) and water (Gehring and Hofmeister, 1994). Maghemite subsequently transforms to hematite ($\alpha\text{-Fe}_2\text{O}_3$) with continuous heating. The conversion temperatures at which this reaction takes place is variable, but is generally completed before reaching 600°C (Gehring and Hofmeister, 1994; Gendler et al., 2005).

Lepidocrocite's low alteration temperature, rapid conversion to a strong ferrimagnet, and subsequent transformation to a weak canted-antiferromagnet when heated leads to a unique HT- χ signature. At present, no other magnetic mineral commonly found in sedimentary rocks have been reported to present this alteration characteristics (Henry, 2007). Hexagonal pyrrhotite also exhibits a unique magnetic signature (Figure 7). Variation in alteration characteristics with changes in magnetic mineralogy and quantity for reservoir sandstones will not obscure the presence of these minerals as the non-uniqueness and complexity of these sandstones will only be apparent from about 300°C .

6 Conclusion

High temperature susceptibility (HT- χ) measurement has been identified as a method of differentiating the oil leg region from the oilwater transition zone (OWTZ) in some petroleum reservoirs. The variation in signature is due to the presence of hexagonal pyrrhotite and/or lepidocrocite at the OWTZ. These two minerals have unique alteration characteristics. Hexagonal pyrrhotite, which has been identified at the OWTZ of shallow hydrocarbon fields (reservoir temperatures $<80^\circ\text{C}$), is preferential precipitated at this zone due to increased microbial activities related to the presence of mobile hydrocarbons and water supplying the required reactants. For deeper petroleum reservoirs ($>80^\circ\text{C}$), lepidocrocite formation has been identified as the main source of the distinct HT- χ signature around the contact. It may also form in shallower settings depending on the balance of the available ions present. Lepidocrocite's precipitation is likely related to increased hydrolysis of hydrocarbon at the OWTZ (Helgeson et al., 1993).

Data availability statement

The raw data supporting the conclusions of this article will be made available by the authors, without undue reservation.

Author contributions

MA, AM, and AF contributed to conception and design of the study. MA carried out the required experiments, organized the database and wrote the first draft of the manuscript. MA, AM, and AF read, revised and approved the submitted version.

Acknowledgments

MA acknowledges receipt of a PhD scholarship from the Petroleum Technology Development Fund (PTDF), Nigeria, and Visiting Fellowships to the Institute for Rock Magnetism (I.R.M.), University of Minnesota. The IRM is a US National Multi-user Facility supported through the Instrumentation and Facilities program of the National Science Foundation, Earth Sciences Division, and by funding from the University of Minnesota. AM acknowledges funding for the SPIN-Lab

References

- Abdulkarim, M. A., Muxworthy, A. R., Fraser, A., Neumaier, M., Hu, P., and Cowan, A. (2022a). Siderite occurrence in petroleum systems and its potential as a hydrocarbon-migration proxy: A case study of the catcher area development and the bittern area, UK North Sea. *J. Petroleum Sci. Eng.* 212, 110248. doi:10.1016/j.petrol.2022.110248
- Abdulkarim, M. A., Muxworthy, A. R., Fraser, A., Sims, M., and Cowan, A. (2022b). Effect of hydrocarbon presence and properties on the magnetic signature of the reservoir sediments of the catcher area development region, UK North Sea. *Front. Earth Sci.* 10, 1–20. doi:10.3389/feart.2022.818624
- Abubakar, R., Muxworthy, A. R., Fraser, A., Sephton, M. A., Watson, J. S., Heslop, D., et al. (2020). Mapping hydrocarbon charge-points in the Wessex Basin using seismic, geochemistry and mineral magnetics. *Mar. Petroleum Geol.* 111, 510–528. doi:10.1016/j.marpetgeo.2019.08.042
- Adegbite, J. O., Belhaj, H., and Bera, A. (2021). Investigations on the relationship among the porosity, permeability and pore throat size of transition zone samples in carbonate reservoirs using multiple regression analysis, artificial neural network and adaptive neuro-fuzzy interface system. *Petroleum Res.* 6, 321–332. doi:10.1016/j.ptlrs.2021.05.005
- Badejo, S. A., Fraser, A. J., Neumaier, M., Muxworthy, A. R., and Perkins, J. R. (2021a). 3D petroleum systems modelling as an exploration tool in mature basins: A study from the Central North Sea UK. *Mar. Petroleum Geol.* 133, 105271. doi:10.1016/j.marpetgeo.2021.105271
- Badejo, S. A., Muxworthy, A., Fraser, A., Stevenson, G., Zhao, X., and Jackson, M. (2021b). Identification of magnetic enhancement at hydrocarbon-fluid contacts. *Bulletin* 105, 1973–1991. doi:10.1306/07062019207
- Badejo, S. A., Muxworthy, A. R., Fraser, A., Neumaier, M., Perkins, J. R., Stevenson, G. R., et al. (2021c). Using magnetic techniques to calibrate hydrocarbon migration in petroleum systems modelling: A case study from the lower tertiary, UK Central North Sea. *Geophys. J. Int.* 227, 617–631. doi:10.1093/gji/ggab236
- Bassez, M. P. (2017). Anoxic and oxic oxidation of rocks containing Fe(II) Mg-silicates and Fe(II)-Monosulfides as source of Fe(III)-Minerals and hydrogen. *Geobiotropy. Orig. Life Evol. Biosph.* 47, 453–480. doi:10.1007/s11084-017-9534-5
- Bera, A., and Belhaj, H. (2016). A comprehensive review on characterization and modeling of thick capillary transition zones in carbonate reservoirs. *J. Unconv. Oil Gas Resour.* 16, 76–89. doi:10.1016/j.juogr.2016.10.001
- Burton, E. A., Machel, H. G., and Qi, J. (1993). “Thermodynamic constraints on anomalous magnetization in shallow and deep hydrocarbon seepage environments,” in *SEPM special publication* (London: SEPM Society for Sedimentary Geology), 193–207. doi:10.2110/pec.93.4910.2110/pec.93.49.0193
- Copestake, P., Sims, A. P., Crittenden, S., Hamar, G. P., Ineson, J. R., Rose, P. T., et al. (2003). “Lower cretaceous,” in *The millennium atlas: Petroleum geology of the central and Northern North Sea*. Editors E. Evans, C. Graham, A. Armour, and

facility from EPSRC (grant EP/P030548/1). We also thank the British Geological Survey for the core samples.

Conflict of interest

The authors declare that the research was conducted in the absence of any commercial or financial relationships that could be construed as a potential conflict of interest.

Publisher's note

All claims expressed in this article are solely those of the authors and do not necessarily represent those of their affiliated organizations, or those of the publisher, the editors and the reviewers. Any product that may be evaluated in this article, or claim that may be made by its manufacturer, is not guaranteed or endorsed by the publisher.

P. Bathurst (The Geological Society of London), 191–211. doi:10.1017/S0016756803218124

Dekkers, M. J. (1989). Magnetic properties of natural pyrrhotite. II. High- and low-temperature behaviour of Jrs and TRM as function of grain size. *Phys. Earth Planet. Interiors* 57, 266–283. doi:10.1016/0031-9201(89)90116-7

Dyar, M. D., Agresti, D. G., Schaefer, M. W., Grant, C. A., and Sklute, E. C. (2006). Mössbauer spectroscopy of Earth and planetary materials. *Annu. Rev. Earth Planet. Sci.* 34, 83–125. doi:10.1146/annurev.earth.34.031405.125049

Eldrett, J., Tripsanas, E., Davis, C., McKie, T., Vieira, M., Osterloff, P., et al. (2015). Sedimentological evolution of Sele formation deep-marine depositional systems of the Central North Sea. *Sp* 403, 63–98. doi:10.1144/SP403.9

Emmerton, S., Muxworthy, A. R., Sephton, M. A., Aldana, M., Costanzo-Alvarez, V., Bayona, G., et al. (2013). Correlating biodegradation to magnetization in oil bearing sedimentary rocks. *Geochimica Cosmochimica Acta* 112, 146–165. doi:10.1016/j.gca.2013.03.008

Fanchi, J. R., Christiansen, R. L., and Heymans, M. J. (2002). Estimating oil reserves of fields with oil/water transition zones. *SPE Reserv. Eval. Eng.* 5, 311–316. doi:10.2118/79210-PA

Fraser, S. I., Robinson, A. M., Johnson, H. D., Underhill, J. R., Kadolsky, D. G. A., Connell, R., et al. (2003). “Upper jurassic,” in *The millennium atlas: Petroleum geology of the central and Northern North Sea*. Editors E. Evans, C. Graham, A. Armour, and P. Bathurst (London: The Geological Society of London), 157–189. doi:10.1017/S0016756803218124

Fu, D., Keech, P. G., Sun, X., and Wren, J. C. (2011). Iron oxyhydroxide nanoparticles formed by forced hydrolysis: Dependence of phase composition on solution concentration. *Phys. Chem. Chem. Phys.* 13, 18523–18529. doi:10.1039/c1cp20188c

Gehring, A. U., and Hofmeister, A. M. (1994). The transformation of lepidocrocite during heating: A magnetic and spectroscopic study. *Clays Clay Minerals* 42, 409–415. doi:10.1346/CCMN.1994.0420405

Gendler, T. S., Shcherbakov, V. P., Dekkers, M. J., Gapeev, A. K., Gribov, S. K., and McClelland, E. (2005). The lepidocrocite-maghemite-haematite reaction chain-I. Acquisition of chemical remanent magnetization by maghemite, its magnetic properties and thermal stability. *Geophys. J. Int.* 160, 815–832. doi:10.1111/j.1365-246X.2005.02550.x

Head, I. M., Gray, N. D., and Larter, S. R. (2014). Life in the slow lane; biogeochemistry of biodegraded petroleum containing reservoirs and implications for energy recovery and carbon management. *Front. Microbiol.* 5, 1–23. doi:10.3389/fmicb.2014.00566

Head, I. M., Larter, S. R., Gray, N. D., Sherry, A., Adams, J. J., Aitken, C. M., et al. (2010). “Handbook of hydrocarbon and lipid microbiology,” in *Handbook of hydrocarbon and lipid microbiology*. Editor K. N. Timmis (Berlin,

Heidelberg: Springer Berlin Heidelberg), 3098–3107. doi:10.1007/978-3-540-77587-4

Helgeson, H. C., Knox, A. M., Owens, C. E., and Shock, E. L. (1993). Petroleum, oil field waters, and authigenic mineral assemblages: Are they in metastable equilibrium in hydrocarbon reservoirs. *Geochimica Cosmochimica Acta* 57, 3295–3339. doi:10.1016/0016-7037(93)90541-4

Henry, B. (2007). “Magnetic mineralogy, changes due to heating,” in *Encyclopedia of geomagnetism and paleomagnetism*. Editors D. Gubbins and E. Herrero-Bervera (Dordrecht: Springer Netherlands), 512–515. doi:10.1007/978-1-4020-4423-6_179

Hirt, A. M., Lanci, L., Dobson, J., Weidler, P., and Gehring, A. U. (2002). Low-temperature magnetic properties of lepidocrocite. *J. Geophys. Res.* 107, 5–1. doi:10.1029/2001jb000242

Hornig, C. S. (2018). Unusual magnetic properties of sedimentary pyrrhotite in methane seepage sediments: Comparison with metamorphic pyrrhotite and sedimentary greigite. *J. Geophys. Res. Solid Earth* 123, 4601–4617. doi:10.1002/2017JB015262

James, M., Bastow, M., Thompson, S., Scotchman, I., and Oygard, K. (2003). “EVANS, D., GRAHAM, C., ARMOUR, A. & BATHURST, P. (editors and compilers) 2003. The Millennium Atlas: Petroleum Geology of the Central and Northern North Sea. 389 pp. London, Bath: Geological Society of London. Price £248 (book plus CD set); book only - £199; CD only - £199; hard covers, large format. ISBN 1 86239 119 X.” in *The millennium atlas: Petroleum geology of the central and Northern North Sea*. Editors P. D. Evans, C. Graham, and A. Armour (London: The Geological Society of London), 140, 487. doi:10.1017/S0016756803218124

James, Z., Sawyers, M., Kenyon-Roberts, S., Stanworth, C., Kugler, K., Kristensen, J., et al. (2003). The millennium atlas: Petroleum geology of the central and Northern North Sea. 389 pp. London, bath: Geological society of London. Price £248 (book plus CD set); book only - £199; CD only - £199; hard covers, large format. ISBN 1 86239 119 X.” in *The millennium atlas: Petroleum geology of the central and Northern North Sea*. Editors P. D. Evans, C. Graham, A. Armour, and P. Bathurst (London: The Geological Society of London), 140, 487. doi:10.1017/S0016756803218124

Johnson, H., Leslie, A. B., Wilson, C. K., Andrews, I., and Cooper, R. M. (2005). Middle jurassic, upper jurassic and lower cretaceous of the UK central and Northern North Sea. British geological Survey research report, RR/03/001. *Br. Geol. Surv.* 55, 1–37.

Jones, E., Jones, R., Ebdon, C., Ewen, D., Milner, P., Plunkett, J., et al. (2003). “Eocene,” in *The millennium atlas: Petroleum geology of the central and Northern North Sea*. Editors D. Evans, C. Graham, A. Armour, and P. Bathurst (London: The Geological Society of London), 261–277.

Kao, S. J., Hornig, C. S., Roberts, A. P., and Liu, K. K. (2004). Carbon-sulfur-iron relationships in sedimentary rocks from southwestern Taiwan: Influence of geochemical environment on greigite and pyrrhotite formation. *Chem. Geol.* 203, 153–168. doi:10.1016/j.chemgeo.2003.09.007

Liu, A., Liu, J., Pan, B., and Zhang, W. X. (2014). Formation of lepidocrocite (γ -FeOOH) from oxidation of nanoscale zero-valent iron (nZVI) in oxygenated water. *RSC Adv.* 4, 57377–57382. doi:10.1039/c4ra08988j

Liu, Q., Liu, Q., Chan, L., Yang, T., Xia, X., and Cheng, T. (2006). Magnetic enhancement caused by hydrocarbon migration in the mawangmiao oil field, jiangnan basin, China. *J. Petroleum Sci. Eng.* 53, 25–33. doi:10.1016/j.petrol.2006.01.010

McKie, T., Rose, P. T. S., Hartley, A. J., Jones, D. W., and Armstrong, T. L. (2015). Tertiary deep-marine reservoirs of the North Sea region: An introduction. *Sp* 403, 1–16. doi:10.1144/SP403.12

Mudge, D. C. (2015). Regional controls on lower tertiary sandstone distribution in the north Sea and NE atlantic margin basins. *Sp* 403, 17–42. doi:10.1144/SP403.5

Pan, Y., Zhu, R., Banerjee, S. K., Gill, J., and Williams, Q. (2000). Rock magnetic properties related to thermal treatment of siderite: Behavior and interpretation. *J. Geophys. Res.* 105, 783–794. doi:10.1029/1999jb900358

Pannekens, M., Kroll, L., Müller, H., Mbow, F. T., and Meckenstock, R. U. (2019). Oil reservoirs, an exceptional habitat for microorganisms. *New Biotechnol.* 49, 1–9. doi:10.1016/j.nbt.2018.11.006

Reynolds, R. L., Fishman, N. S., Wanty, R. B., and Goldhaber, M. B. (1990). Iron sulfide minerals at Cement oil field, Oklahoma: Implications for magnetic detection of oil fields. *Geol. Soc. Am. Bull.* 102, 368–380. doi:10.1130/0016-7606(1990)102<0368:ismaco>2.3.co;2

Ritchie, A. L., Hodzic, M., Brain, J., Coogan, S., Khan, S., McClean, S., et al. (2011). *Bittern further developed through integration*. UK: Devex.

Roberts, A. P. (2015). Magnetic mineral diagenesis. *Earth-Science Rev.* 151, 1–47. doi:10.1016/j.earscirev.2015.09.010

Roberts, A. P., and Turner, G. M. (1993). Diagenetic formation of ferrimagnetic iron sulphide minerals in rapidly deposited marine sediments, South Island, New Zealand. *Earth Planet. Sci. Lett.* 115, 257–273. doi:10.1016/0012-821X(93)90226-Y

Robertson, J., Gouly, N. R., and Swarbrick, R. E. (2013). Overpressure distributions in Palaeogene reservoirs of the UK Central North Sea and implications for lateral and vertical fluid flow. *Pg* 19, 223–236. doi:10.1144/petgeo2012-060

Rochette, P., Fillion, G., Mattéi, J. L., and Dekkers, M. J. (1990). Magnetic transition at 30–34 kelvin in pyrrhotite: Insight into a widespread occurrence of this mineral in rocks. *Earth Planet. Sci. Lett.* 98, 319–328. doi:10.1016/0012-821X(90)90034-U

Stevens, J. G., Khasanov, A. M., Miller, J. W., Pollak, H., and Li, Z. (2005). Mössbauer mineral handbook. 3rd editio. Asheville: Mossbauer Effect Data Center.

Stewart, S. A. (1996). Tertiary extensional fault systems on the Western margin of the North Sea Basin. *Pg* 2, 167–176. doi:10.1144/petgeo.2.2.167

Surlyk, F., Dons, T., Clausen, C., and Higham, J. (2003). “Upper cretaceous,” in *The millennium atlas: Petroleum geology of the central and Northern North Sea*. Editors D. Evans, C. Graham, A. Armour, and P. Bathurst (London: The Geological Society of London), 213–233.

Tamanna, M. S., Bhullar, A. G., and Ward, C. (2013). “Identification of seismic facies and effect of seismic data quality on hydrocarbon distribution in Pict field,” in *Central North Sea* (London, United Kingdom: AAPG).